Dynamic structure factor of ultracold Bose and Fermi gases in optical lattices

Robert Roth

Institut für Kernphysik, Technische Universität Darmstadt, 64289 Darmstadt, Germany

Keith Burnett

Clarendon Laboratory, University of Oxford, Parks Road, Oxford OX1 3PU, United Kingdom

Abstract. We investigate the dynamic structure factor of atomic Bose and Fermi gases in one-dimensional optical lattices at zero temperature. The focus is on the generic behaviour of $S(k,\omega)$ as function of filling and interaction strength with the aim of identifying possible experimental signatures for the different quantum phase transitions. We employ the Hubbard or Bose-Hubbard model and solve the eigenvalue problem of the Hamiltonian exactly for moderate lattice sizes. This allows us to determine the dynamic structure factor and other observables directly in the phase transition regime, where approximation schemes are generally not applicable. We discuss the characteristic signatures of the various quantum phases appearing in the dynamic structure factor and illustrate that the centroid of the strength distribution can be used to estimate the relevant excitation gaps. Employing sum rules, these quantities can be evaluated using ground state expectation values only. Important differences between bosonic and fermionic systems are observed, e.g., regarding the origin of the excitation gap in the Mott-insulator phase.

PACS numbers: 03.75.Lm, 03.75.Ss

1. Introduction

Ultracold atomic gases in optical lattices have proven to be an unique experimental tool to explore the rich physics of quantum phase transitions. Since the first experimental observation of the superfluid to Mott-insulator transition in an ultracold Bose gas contained in a three-dimensional optical lattice [1], the theoretical and experimental activity in this field has increased dramatically. Recently, the superfluid to Mott-insulator phase transition was also confirmed in one-dimensional lattices [2]. From the experimental point of view these systems offer a remarkable degree of experimental control: lattice depth and topology, interaction strengths, and filling factors can be adjusted in a wide range. Furthermore one has the choice between purely bosonic or fermionic single- or multi-component systems as well as systems of mixed statistics. At the same time the diagnostic tools are outstanding. The matter wave interference pattern after release from the lattice already provides a wealth of information. The dynamic response of the system can be probed, e.g., by tilting or modulating the lattice potential [3, 2]. Bragg spectroscopy [4, 5] provides another powerful tool to access dynamic properties.

Also from the theoretical point of view these systems are appealing. They open a window to correlation dominated phenomena far beyond the mean-field regime. The most striking ramification of the influence of correlations are the different quantum phases appearing in Bose and Fermi gases in lattices. For sufficiently deep lattice potentials the single-band Hubbard or Bose-Hubbard model is well suited to study all these phenomena. Besides the superfluid to Mott-insulator transition for bosonic atoms in an optical lattice [6] many other phenomena have been successfully described within the Bose-Hubbard model. Presently a lot of attention is devoted to fermionic systems and Bose-Fermi mixtures in lattices [7, 8, 9, 10] with the intention to investigate pairing and fermionic superfluidity in lattice systems.

The aim of this paper is to systematically investigate the dynamic structure factor of bosonic and fermionic lattice systems within the (Bose-) Hubbard model. The dynamic structure factor, which is directly accessible in experiment, e.g., through two-photon Bragg spectroscopy [4, 5, 11], fully characterises the density-density response. It provides detailed insight into the spectrum of elementary excitations and into the role correlations for the dynamics of the system. A significant amount of work has been done for weakly interacting atomic gases in optical lattices using the Bogoliubov approach [12, 13]. In contrast to these studies we are aiming at the regime of strong interactions and correlations which is not accessible within mean-field or Bogoliubov-type models [14]. In order to be able to describe the system throughout the whole phase diagram, we perform an exact numerical solution of the eigenvalue problem of the Hubbard Hamiltonian [15, 16, 10]. This enables us to track the change of the dynamic structure factor through the phase transition and identify signatures of the different quantum phases.

After setting the formal stage in section 2 we discuss our results for the dynamic structure factor of the single-component zero-temperature Bose gas in a one-dimensional optical lattice in section 3. In section 4 we transfer this to a two-component Fermi gas and investigate the behaviour of the dynamic density and spin structure factor in the presence of repulsive and attractive interactions. Section 5 summarises our findings.

2. Hubbard models and the dynamic structure factor

2.1. Bose-Hubbard and Fermi-Fermi-Hubbard model

A single-component Bose gas in a translationally invariant one-dimensional lattice of sufficient depth is described by the single-band Bose-Hubbard Hamiltonian [6, 16]

$$\hat{\mathrm{H}}^{\mathrm{B}} = -J \sum_{i=1}^{I} (\hat{\mathrm{a}}_{i+1}^{\dagger} \hat{\mathrm{a}}_i + \mathrm{H.a.}) + \frac{V}{2} \sum_{i=1}^{I} \hat{\mathrm{n}}_i (\hat{\mathrm{n}}_i - 1) \,, \tag{1}$$

where $\hat{\mathrm{a}}_i^{\dagger}$ creates a boson in the lowest Wannier state localised at site i and $\hat{\mathrm{n}}_i = \hat{\mathrm{a}}_i^{\dagger} \hat{\mathrm{a}}_i$ is the associated occupation number operator. The first term describes the hopping between adjacent sites with a tunnelling matrix element J. Throughout this paper periodic boundary conditions are assumed, i.e., the hopping term connects the first and the last site of the lattice. The second term in (1) introduces an on-site two-body interaction of strength V.

We exactly solve the matrix eigenvalue problem of the Hamiltonian in a basis of Fock states $|\{n_1, ..., n_I\}_{\alpha}^{\mathrm{B}}\rangle$ with $n_i = 0, 1, 2, ...$ The index $\alpha = 1, ..., D$ labels the different compositions of occupation numbers $\{n_1, ..., n_I\}_{\alpha}^{\mathrm{B}}$ for fixed total particle number $N = \sum_{i=1}^{I} n_i$. The resulting basis dimension is $D = (N + I - 1)!/[N!(I - 1)!]$. Through a powerful Lanczos-type algorithm we compute up to 2500 energy eigenvalues E_ν at the lower end of the spectrum. The corresponding eigenvectors $C_{\alpha}^{(\nu)}$ determine the eigenstates

$$|\Psi_{\nu}^{\mathrm{B}}\rangle = \sum_{\alpha=1}^{D} C_{\alpha}^{(\nu)} \, |\{n_1, ..., n_I\}_{\alpha}^{\mathrm{B}}\rangle \,, \tag{2}$$

which are the starting point for the calculation of all relevant observables, like mean occupation numbers, occupation number fluctuations, density matrices, and the dynamic structure factor.

The analogous model for a two-component system of fermionic atoms in a one-dimensional lattice is defined by the (Fermi-Fermi-) Hubbard Hamiltonian

$$\hat{\mathrm{H}}^{\mathrm{FF}} = -J \sum_{i=1}^{I} (\hat{\mathrm{a}}_{\uparrow i+1}^{\dagger} \hat{\mathrm{a}}_{\uparrow i} + \mathrm{H.a.}) - J \sum_{i=1}^{I} (\hat{\mathrm{a}}_{\downarrow i+1}^{\dagger} \hat{\mathrm{a}}_{\downarrow i} + \mathrm{H.a.}) + V \sum_{i=1}^{I} \hat{\mathrm{n}}_{\uparrow i} \hat{\mathrm{n}}_{\downarrow i} \,, \tag{3}$$

where $\hat{\mathrm{a}}_{\uparrow i}^{\dagger}$ and $\hat{\mathrm{a}}_{\downarrow i}^{\dagger}$ are creation operators for a fermionic atom of component $\uparrow$ and $\downarrow$, respectively, localised at site i. $\hat{\mathrm{n}}_{\uparrow i}$ and $\hat{\mathrm{n}}_{\downarrow i}$ are the associated occupation number operators. The first two terms describe the nearest neighbour hopping with a tunnelling matrix element J assumed to be equal for the two components. The last term gives the on-site interaction between two atoms of different components with strength V. A on-site interaction between atoms of the same component is excluded from the outset by restricting the model space to a single band.

Again we use a complete basis of Fock states and perform an exact matrix diagonalisation of the Hamiltonian. For a single fermionic component with N particles, a basis of Fock states $|\{n_1, ..., n_I\}_{\alpha}^{\mathrm{F}}\rangle$ is given by all possible arrangements of N sites with $n_i = 1$ and $(I - N)$ sites with $n_i = 0$. The dimension $D = I!/[N!(I - N)!]$ of this basis is much smaller than for a corresponding bosonic system, since the Pauli principle forbids multiply occupied sites. The Fock basis of a two-component system is given by the direct product of all possible combinations of the single-component basis states $|\{n_1, ..., n_I\}_{\alpha}^{\mathrm{F}\uparrow}\rangle \otimes |\{n_1, ..., n_I\}_{\beta}^{\mathrm{F}\downarrow}\rangle$. The solution of the matrix eigenvalue problem of the Hamiltonian in this basis yields eigenstates of two-component fermion system of the form

$$|\Psi_{\nu}^{\mathrm{FF}}\rangle = \sum_{\alpha=1}^{D_\uparrow} \sum_{\beta=1}^{D_\downarrow} C_{\alpha\beta}^{(\nu)} \, |\{n_1, ..., n_I\}_{\alpha}^{\mathrm{F}\uparrow}\rangle \otimes |\{n_1, ..., n_I\}_{\beta}^{\mathrm{F}\downarrow}\rangle \,. \tag{4}$$

2.2. Dynamic structure factor

In order to characterise and investigate the dynamic density-density response of bosonic or fermionic lattice systems to an external probe, which delivers a momentum k and an energy ω, we employ the dynamic structure factor $S(k,\omega)$. It is assumed that the coupling between probe and system is sufficiently weak to render a linear response treatment applicable. At zero temperature the dynamic structure factor is defined as [17]

$$S(k,\omega) = \sum_{\nu} |\langle \Psi_\nu | \hat{\rho}_k^\dagger | \Psi_0 \rangle|^2 \, \delta(\omega - E_{\nu 0}) \, , \tag{5}$$

where $|\Psi_\nu\rangle$ are the eigenstates of the many-body Hamiltonian and $E_{\nu 0} = E_\nu - E_0$ are the excitation energies relative to the ground state. In this section we omit any reference to the bosonic or fermionic system, since the formal steps are identical for both.

The operator $\hat{\rho}_k^\dagger$ describes the way the external probe couples to the system. In the case of the dynamic structure factor it creates an excitation with momentum k by promoting particles from a state with quasimomentum q to a state with quasimomentum $q + k$. In the language of second quantisation this reads [17]

$$\hat{\rho}_k^\dagger = \sum_{q=0}^{I-1} \hat{\mathrm{c}}_{q+k}^\dagger \hat{\mathrm{c}}_q \, , \tag{6}$$

where the $\hat{\mathrm{c}}_q^\dagger$ are creation operators associated with quasimomentum eigenstates, i.e., Bloch states. Within the Hubbard model the $\hat{\mathrm{c}}_q^\dagger$ can be rephrased in terms of the creation operators $\hat{\mathrm{a}}_i^\dagger$ with respect to the localised Wannier states through

$$\hat{\mathrm{c}}_q = \frac{1}{\sqrt{I}} \sum_{i=1}^{I} \mathrm{e}^{\mathrm{i}(2\pi/I)\, q\, i} \, \hat{\mathrm{a}}_i \, . \tag{7}$$

We employ reduced units for the quasimomenta such that only integer values of q appear. The first Brillouin zone contains I different quasimomentum states which are labelled $q = 0, ..., I-1$ for convenience. The quasimomenta in standard units are given by $2\pi\, q/(aI)$, where a is the lattice spacing. Inserting (7) into equation (6) leads to the simple expression

$$\hat{\rho}_k^\dagger = \sum_{i=1}^{I} \mathrm{e}^{-\mathrm{i}(2\pi/I)\, k\, i} \, \hat{\mathrm{n}}_i \, . \tag{8}$$

This form clearly shows that the operator $\hat{\rho}_k^\dagger$ is related to a periodic density modulation with quasimomentum k. In order to isolate the fluctuating part, one might subtract the mean occupation numbers $\bar{n}_i$ for the ground state from the occupation number operator $\hat{\mathrm{n}}_i$ in (8). However, this affects only the trivial $k = 0$ behaviour of the dynamic structure factor.

The matrix elements $\langle \Psi_\nu | \hat{\rho}_k^\dagger | \Psi_0 \rangle$ entering into the dynamic structure factor can be calculated explicitly for each excited state $|\Psi_\nu\rangle$ obtained by the diagonalisation of the Hubbard Hamiltonian. Using the expansion (2) of the eigenstates in terms of Fock states we obtain

$$\langle \Psi_\nu | \hat{\rho}_k^\dagger | \Psi_0 \rangle = \sum_{i=1}^{I} \mathrm{e}^{-\mathrm{i}(2\pi/I)\, k\, i} \sum_{\alpha,\beta=1}^{D} C_\alpha^{(\nu)\star} C_\beta^{(0)} \langle \{n_1 ... n_I\}_\alpha | \, \hat{\mathrm{n}}_i \, | \{n_1 ... n_I\}_\beta \rangle \tag{9}$$

$$= \sum_{i=1}^{I} \mathrm{e}^{-\mathrm{i}(2\pi/I)\, k\, i} \sum_{\alpha=1}^{D} C_\alpha^{(\nu)\star} C_\alpha^{(0)} n_i^{(\alpha)} \, . \tag{10}$$

Since we only compute the lowest $\nu_{\max}$ eigenstates by the Lanczos procedure, the excitation energy $E_{\nu_{\max} 0}$ of the highest eigenstate limits the ω up to which the structure factor is

determined. By checking the sum rules (cf. section 2.3) we make sure that all relevant contributions are contained in this range.

So far, we have discussed a single component system. In a two-component system, the probe can couple to the two components in different ways. If the probe does not distinguish the two components, then the operator of the total on-site occupation number $\hat{n}_{\uparrow i} + \hat{n}_{\downarrow i}$ is the relevant quantity and enters into the definition of the total density fluctuation operator [11]

$$\hat{\rho}^{\dagger}_{\mathrm{D}k} = \sum_{i=1}^{I} \mathrm{e}^{-\mathrm{i}(2\pi/I)\,k\,i}\ (\hat{n}_{\uparrow i} + \hat{n}_{\downarrow i})\ . \tag{11}$$

With equation (5) this defines the dynamic density structure factor $S_{\mathrm{D}}(k,\omega)$. If the probe, on the other hand, couples to the total on-site spin, then the difference between the two occupation number operators $\hat{n}_{\uparrow i} - \hat{n}_{\downarrow i}$ is decisive and leads to the spin fluctuation operator

$$\hat{\rho}^{\dagger}_{\mathrm{S}k} = \sum_{i=1}^{I} \mathrm{e}^{-\mathrm{i}(2\pi/I)\,k\,i}\ (\hat{n}_{\uparrow i} - \hat{n}_{\downarrow i}) \tag{12}$$

and the associated dynamic spin structure factor $S_{\mathrm{S}}(k,\omega)$. Possible ways of measuring these quantities in ultracold atomic gases are discussed in ref. [11].

2.3. Sum Rules

Sum rules provide an outstanding tool in connection with the dynamic structure factor [12]. They relate the moments of the dynamic structure factor to ground state expectation values of different operators. The simplest sum rule relates the dynamic structure factor $S(k,\omega)$ to the static structure factor $S(k)$. The integral of $S(k,\omega)$ over ω, i.e., the zeroth moment of the dynamic structure factor, is proportional to the static structure factor

$$\int \mathrm{d}\omega\ S(k,\omega) = \sum_{\nu} |\langle\Psi_\nu|\,\hat{\rho}^{\dagger}_{k}\,|\Psi_0\rangle|^2 \stackrel{!}{=} \langle\Psi_0|\,\hat{\rho}^{\dagger}_{k}\hat{\rho}_{k}\,|\Psi_0\rangle \equiv NS(k)\ . \tag{13}$$

The first equality follows immediately from the definition of the dynamic structure factor (5). The equivalence of the second and the third expression can be easily shown by making use of the completeness of the eigenstates $|\Psi_\nu\rangle$ of the Hamiltonian. Inserting a unit operator $\hat{1} = \sum_\nu |\Psi_\nu\rangle\langle\Psi_\nu|$ between the two fluctuation operators in the third expression immediately leads to the second expression. In view of this relation it is convenient to define a normalised dynamic structure factor $\bar{S}(k,\omega) = S(k,\omega)/(NS(k))$, whose zeroth moment equals 1 independent of k.

The first moment of the dynamic structure factor obeys the energy-weighted or f sum-rule. For Hubbard-type Hamiltonians with next neighbour hopping one finds

$$\int \mathrm{d}\omega\ \omega\ S(k,\omega) = \sum_{\nu} E_{\nu 0}\ |\langle\Psi_\nu|\,\hat{\rho}^{\dagger}_{k}\,|\Psi_0\rangle|^2 \stackrel{!}{=} [\cos(2\pi k/I) - 1]\ \langle\Psi_0|\,\hat{\mathrm{T}}\,|\Psi_0\rangle \equiv f(k)\ , \tag{14}$$

where $\hat{\mathrm{T}} = -J\sum_{i=1}^{I}(\hat{a}^{\dagger}_{i+1}\hat{a}_i + \hat{a}^{\dagger}_i\hat{a}_{i+1})$ is the kinetic energy part of the Hamiltonian. Again, the second term follows directly from the definition of the dynamic structure factor. The equivalence of the second and third expression can be proven by considering the ground state expectation value of the double-commutator $[[\hat{\rho}_k, \hat{\mathrm{H}}], \hat{\rho}^{\dagger}_k]$. Notice, the explicit evaluation of the double-commutator for the Hubbard Hamiltonian leads to a term $2\,[\cos(2\pi k/I) - 1]\,\hat{\mathrm{T}}$ in contrast to the usual expression for homogeneous Bose or Fermi gases [17].

We will make use of these sum rules in two different ways. First, we will check the numerical results for the dynamic structure factor by computing the moments of the structure factor and the corresponding ground state expectation values independently. Thus we make sure that the truncated set of excited states that was obtained numerically, includes all states

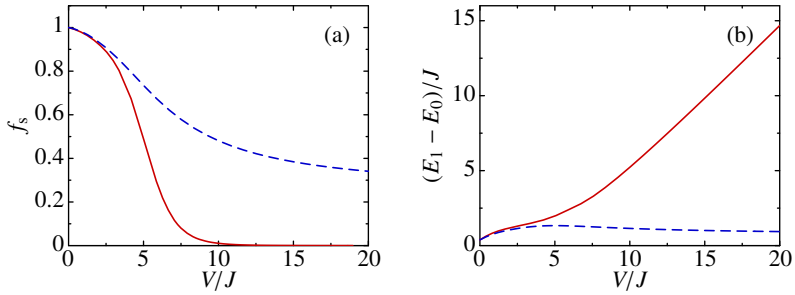

Figure 1. (a) Superfluid fraction f_s as function of the interaction strength V/J [16, 15] for a commensurate system with $I = N = 10$ (——) and for non-commensurate filling $I = 10, N = 8$ (– – –). (b) Energy gap between ground state and first excited state for the same two cases.

which contribute to the dynamic structure factor, i.e., which have non-vanishing matrix elements $\langle\Psi_\nu|\hat{\rho}_k^\dagger|\Psi_0\rangle$. Secondly, we can utilise sum rules to determine integral properties of the dynamic structure factor without computing excited states explicitly. We can, for example, determine the energy of the centroid of the strength distribution, given by the ratio of the first and the zeroth moment of $S(k,\omega)$, using ground state expectation values alone. We will come back to this point at the end of section 3.

3. Single-component Bose gas

The properties of the single-component Bose gas in the presence of repulsive interactions have been studied in detail experimentally as well as theoretically. For commensurate filling factors a quantum phase transition from a superfluid at low values of V/J to a Mott-insulator phase at large V/J appears. For an infinite one-dimensional lattice, Monte Carlo calculations [18] and strong -coupling expansion methods [19] predict a critical interaction strength $(V/J)_{\rm crit} \approx 4.65$ for the superfluid to Mott-insulator transition at $N/I = 1$. This is consistent with the recent experimental observation of the Mott-insulator transition in one-dimensional systems [2]. We have performed explicit calculations of the superfluid fraction in finite systems via the phase stiffness [16, 15]. The behaviour of the superfluid weight f_s and of the energy gap between ground state and first excited state for a lattice with $I = 10$ sites are summarised in figure 1. For commensurate filling ($N = 10$) the superfluid fraction decreases rapidly and a linearly growing energy gap emerges. For incommensurate filling ($N = 8$) the superfluid fraction stays finite and the energy gap between ground and first excited state remains small. A detailed analysis of these properties as well as other observables was presented in [16].

Our aim is to investigate the change of the dynamic structure factor $S(k,\omega)$ throughout the whole phase diagram, i.e., for different interaction strengths V/J and fillings N/I. Different characteristic behaviours might serve as an easily accessible experimental signature to identify the various quantum phases.

Figure 2 summarises our results for the normalised dynamic structure factor $\bar{S}(k,\omega) = S(k,\omega)/(NS(k))$ of a single-component Bose gas with different interaction strengths V/J in a lattice with $I = 10$ sites. For the sake of clarity the δ-function appearing in the definition (5) of the structure factor is smoothed out, i.e., it is replaced by a narrow Gauss function

$$\delta(\omega - E_{\nu 0}) \to \frac{1}{\sqrt{2\pi}\Delta} \exp\left[-\frac{(\omega - E_{\nu 0})^2}{2\Delta^2}\right] \tag{15}$$

with a width parameter $\Delta/J = 0.2$ (for the fermionic systems discussed in section 4 we use

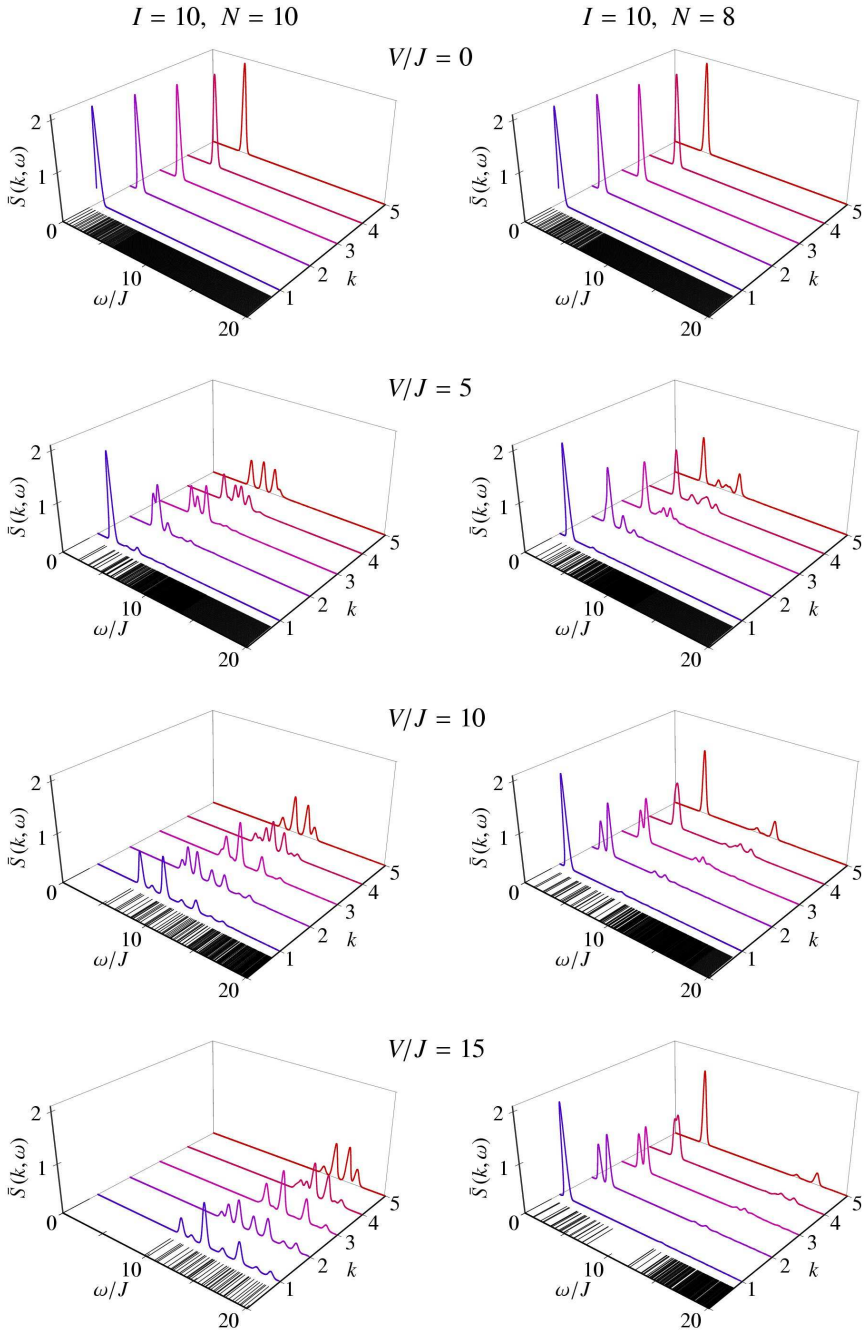

Figure 2. Normalised dynamic structure factor $\bar{S}(k,\omega)$ for a single-component Bose gas in a one-dimensional lattice with $I = 10$ sites. The plots in the left hand column correspond to a commensurate filling with $N = 10$, the one on the right hand side are for incommensurate filling with $N = 8$. The interaction parameters for the different rows are $V/J = 0$, 5, 10, and 15 (from top to bottom). The bars at the forward edge of each plot represent the excitation spectrum, i.e. the possible values of $E_{\nu 0}$.

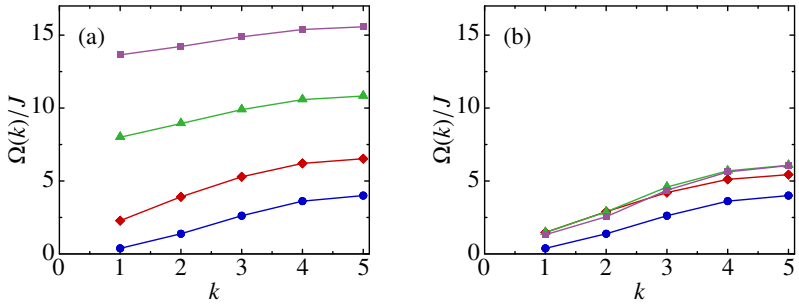

Figure 3. Position of the centroid (16) of the dynamic structure factor as function of k for a single-component Bose gas with (a) $N = 10$ particles and (b) $N = 8$ particles, resp., in a $I = 10$ lattice. The interaction strengths are $V/J = 0$ (●), 5 (♦), 10 (▲), and 15 (■). The points are connected by straight lines to guide the eye.

$\Delta/J = 0.12$). Each of the curves shown in the individual plots corresponds to a different value of the quasimomentum transfer k. Only the non-trivial values $q = 1, 2, ..., I/2$ are shown. For $q = 0$ the structure factor vanishes for $\omega > 0$ as can be seen from equation (5). Furthermore, due to time-reversal invariance the structure factors for $-q$ and q are identical. In addition to the dynamic structure factor each of the plots shows the excitation spectrum as a sequence of levels along the ω-axis.

The plots in the left hand column of figure 2 show the dynamic structure factor for commensurate filling $N = I = 10$. In the absence of interactions (upper plot) the excitation strength for each quasimomentum is concentrated in a single peak at low ω. The peak shifts slightly towards larger excitation energies when the quasimomentum transfer k is increased. In the presence of interactions the excitation strength fragments and spreads over a considerable range of excitation energies ω [20]. This is caused by the change of the structure of the eigenstates which leads to non-vanishing matrix elements $\langle \Psi^{\mathrm{B}}_{\nu} | \hat{\rho}^{\dagger}_{k} | \Psi^{\mathrm{B}}_{0} \rangle$ for several excited states.

A more significant change of $S(k, \omega)$ results from the emergence of a gap in the energy spectrum as soon as one enters the Mott-insulator phase. Starting from $V/J \gtrsim 5$ there is a gap between ground state and first excited state which grows linearly with V/J (cf. figure 1). Hence, there are no low-lying excited states and therefore no low-lying contributions to the dynamic structure factor within the Mott-insulator phase. The excitation strength, which is carried by states just above the energy gap, is pushed towards large ω as the gap expands. The plots for $V/J = 10$ and 15 in figure 2 demonstrate this mechanism.

This can be compared to the behaviour of the dynamic structure factor for a system with non-commensurate filling ($I = 10$, $N = 8$) as depicted in the right hand column of figure 2. As before, the strength is concentrated in a single low-energy peak for the noninteracting system. However, with increasing V/J the dominant part of the strength remains at small ω since there is no gap between ground and first excited state. Nevertheless, a small contribution results from higher lying states which moves to larger ω with increasing V/J. Interestingly, for strongly repulsive interactions, e.g. $V/J = 15$, the spectrum shows a gap at relatively large excitation energies $E_{\nu 0}/J \approx 10$ and the high-lying strength is carried by states just above this gap.

The gross structural changes of $S(k, \omega)$ discussed above are well represented by the position of the centroid of the strength distribution as function of k

$$\Omega(k) = \frac{\int \mathrm{d}\omega \; \omega \, S(k, \omega)}{\int \mathrm{d}\omega \, S(k, \omega)} = \int \mathrm{d}\omega \; \omega \, \bar{S}(k, \omega) = \frac{f(k)}{N S(k)} \,, \tag{16}$$

which is the ratio of the energy-weighted sum rule $f(k)$ defined in equation (14) and the static structure factor $NS(k)$ given by (13). By using the sum-rule identities given in section 2.3, the position of the centroid can be expressed in terms of ground state expectation values only. Hence the sum rules enable us to draw conclusions about the structure of the excitation spectrum once we know the ground state. Obviously this is of great practical importance, we do not have to compute the full excitation spectrum if we are interested in gross properties like $\Omega(k)$.

Figure 3 depicts the position of the centroid as function of k for different interaction parameters V/J and commensurate as well as non-commensurate filling. In general $\Omega(k)$ decreases with decreasing k, however, its minimum value and its behaviour in the limit of small k is crucial. As long as the system is in the superfluid phase, $\Omega(k)$ tends towards zero for in the limit of small k. Only within the Mott-insulator phase, i.e., for $V/J \gtrsim 5$ and commensurate filling, the position of the centroid tends to a finite value for $k \to 0$. The minimum value of $\Omega(k)$ can be used as an estimate for the excitation gap, which, for the bosonic system, coincides with the gap in the excitation spectrum.

4. Two-component Fermi gas

The qualitative behaviour of the dynamic structure factor for a Bose gas in the lattice can be largely understood from the structure of the excitation spectrum alone. This is not the case for two-component Fermi gases, where the transition matrix elements $\langle \Psi_\nu^{\mathrm{FF}} | \hat{\rho}_k^\dagger | \Psi_0^{\mathrm{FF}} \rangle$ play a decisive role.

4.1. Repulsive interactions

We first consider the case of repulsive inter-component interactions. For $N_\uparrow = N_\downarrow = I/2$, i.e., half-filling of the band, there exists a (Hubbard-) Mott-insulator phase similar to the bosonic system. The one-dimensional Hubbard model at exactly half-filling is special in many respects. It is well known [21] that there exists a mapping between the charge or density and the spin sector of the model. By performing a gauge transformation $\hat{\mathrm{a}}_{\uparrow i}^\dagger \to (-1)^i \hat{\mathrm{a}}_{\uparrow i}$ on one of the components the density observables (e.g. the density structure factor) of the Hubbard model with repulsive interactions $V > 0$ are mapped onto the corresponding spin observables (e.g. the spin structure factor) of a system with attractive interaction $-V$ and vice versa. However, this symmetry does not hold away from half-filling.

In the following we investigate the two-component Fermi gas with repulsive interactions at half-filling of the band ($I = 10$, $N_\uparrow = N_\downarrow = 5$) and for particle numbers away from half-filling ($I = 10$, $N_\uparrow = N_\downarrow = 4$) and compare with the bosonic systems of section 3. The energy spectra and the normalised dynamic density structure factors $\bar{S}_{\mathrm{D}}(k,\omega) = S_{\mathrm{D}}(k,\omega)/[(N_\uparrow + N_\downarrow) S_{\mathrm{D}}(k)]$ for the two-component Fermi gas are summarised in figure 4.

The energy spectrum at half-filling develops a gap with increasing strength of the repulsive interaction (cf. left hand column of figure 4). In contrast to the bosonic system at commensurate filling, the gap does not emerge between ground and first excited state but at relatively large excitation energies of $E_{\nu 0}/J \approx 5$. Therefore a significant number of states remains below the gap, and it is a priori not clear whether these contribute to the dynamic structure factor or not. The explicit calculation of $S_{\mathrm{D}}(k,\omega)$ reveals a behaviour similar to the bosonic system at commensurate filling: The strength is shifted towards larger ω with increasing interaction strength V/J. As the gap appears, only those states above the gap contribute to the structure factor. All states below the gap possess vanishing transition matrix elements $\langle \Psi_\nu^{\mathrm{FF}} | \hat{\rho}_{\mathrm{D}k}^\dagger | \Psi_0^{\mathrm{FF}} \rangle$ and, therefore, do not contribute. Hence, the mechanism which

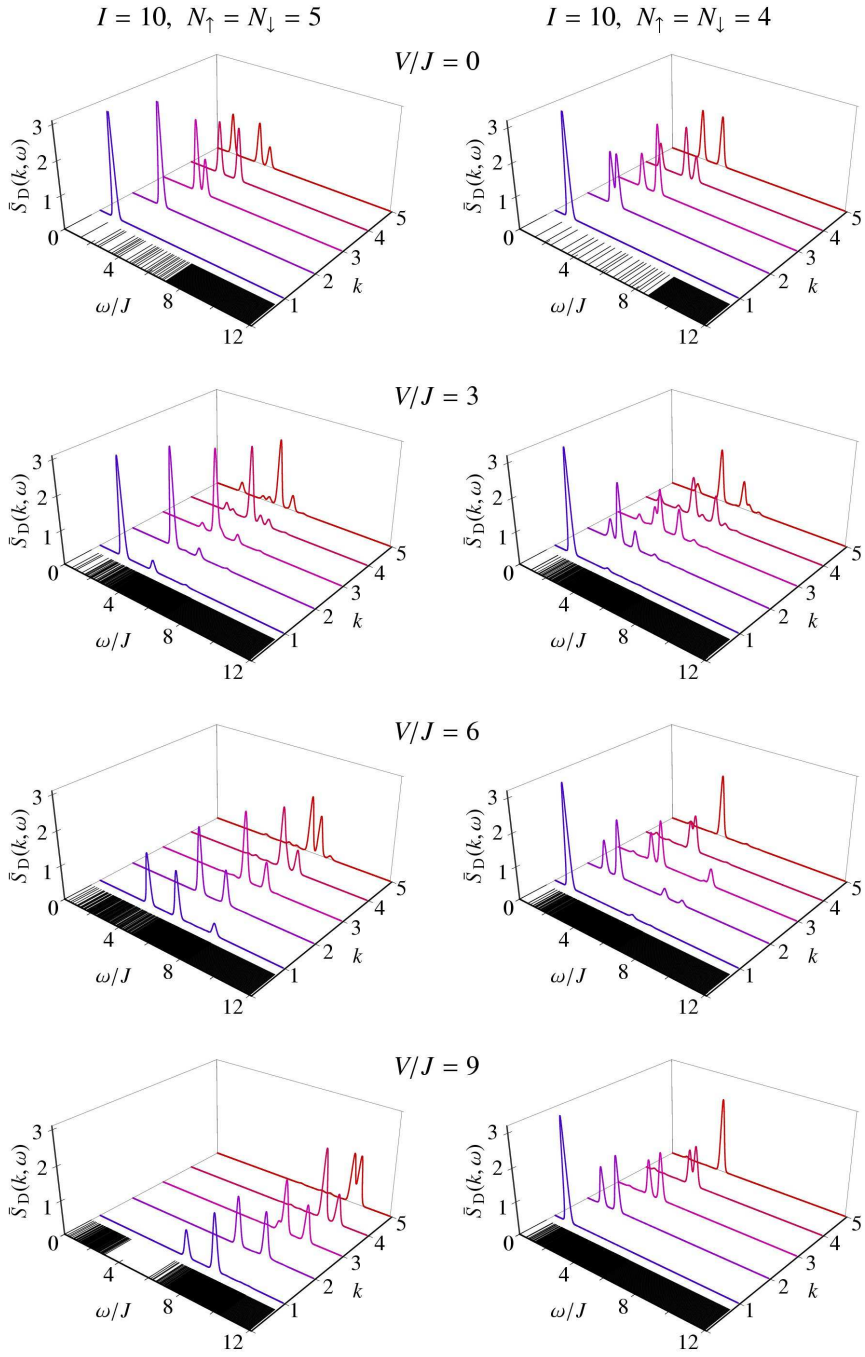

Figure 4. Normalised dynamic density structure factor $\bar{S}_{\rm D}(k,\omega)$ for a two-component Fermi gas with repulsive interactions in a $I = 10$ lattice. The plots in the left hand column show the half-filling case $N_\uparrow = N_\downarrow = 5$, the ones in the right hand column are for $N_\uparrow = N_\downarrow = 4$. The interaction parameters for the different rows are $V/J = 0$, 3, 6, and 9 (from top to bottom). The bars at the forward edge of each plot represent the excitation spectrum, i.e. the possible values of $E_{\nu 0}$.

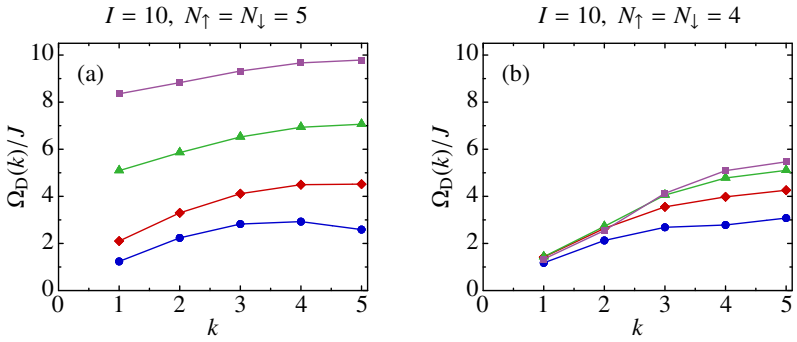

Figure 5. Position of the centroid $\Omega_D(k)$ of the dynamic density structure factor as function of k for a two-component Fermi gas with $N_\uparrow = N_\downarrow = 5$ (a) and $N_\uparrow = N_\downarrow = 4$ (b), resp., in a $I = 10$ lattice. Results are shown for repulsive interactions with $V/J = 0$ (●), 3 (♦), 6 (▲), and 9 (■). The points are connected by straight lines to guide the eye.

generates the density excitation gap is more complicated than for the bosonic system, where it was a simple consequence of the gap in the eigenspectrum.

For systems away from half-filling (right hand column in figure 4), no corresponding gap develops in the energy spectrum. Similar to the non-commensurate bosonic system, the dominant strengths remains at low excitation energies independent of the interaction strength V/J and only a few marginal peaks are shifted to higher ω.

As for the bosonic system, these observations can be quantified in terms of centroid $\Omega_D(k)$ of the dynamic density structure factor $S_D(k, \omega)$. The plots in figure 5 display the position of the centroid as function of k for repulsive interactions of different strengths. At half-filling the centroid shifts towards larger energy transfers with increasing V/J. As for the bosonic system, the k-dependence of $\Omega_D(k)$ can serve as an indicator for the insulating state. If k is decreased towards zero, then the centroid tends to zero in the conducting phase. In the Mott-insulator phase, however, it remains at a finite value which grows linearly with increasing V/J. Again we point out that this behaviour is non-trivial in the fermionic case, it is not simply a consequence of the structure of the energy spectrum. Many states exist below the gap, however, they do not contribute to the dynamic density structure factor. This entails that the excitation gap, i.e., the minimum energy transfer ω required to excite a density fluctuation, is significantly larger than the gap in the spectrum of the Hamiltonian.

Away from half-filling (right panel in figure 5) the position of the centroid always tends towards $\Omega_D(k)/J \approx 0$ for $k \to 0$. This is consistent with our findings for the single-component Bose gas. Hence, the Mott-insulator leaves a clear and general signature in the dynamic density structure factor, which is directly accessible to experiment and allows a distinction from conducting or superfluid phases.

4.2. Attractive interactions

Finally, we address the case of attractive interactions in the two-component Fermi system. This case is of particular interest in view of pairing and superconductivity in these lattice systems.

For half-filling the properties of the gas with attractive interactions can be deduced from the repulsive case on the basis of the spin-density mapping discussed in section 4.1. Its simplest ramification is that the excitation spectrum of a two-component Fermi system with attractive interactions $V < 0$ is *identical* to a system with a repulsive interaction of strength

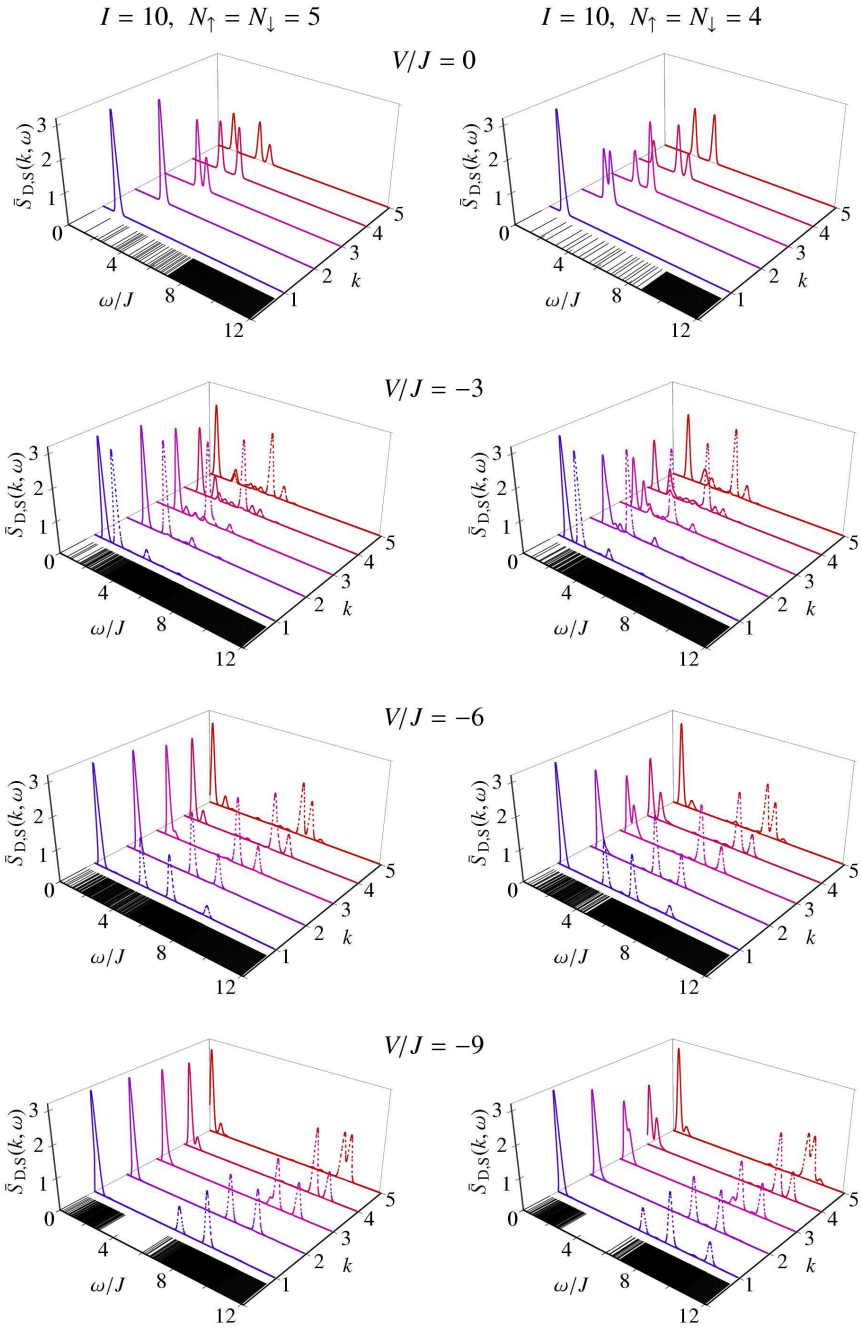

Figure 6. Normalised dynamic density structure factor $\bar{S}_{\mathrm{D}}(k,\omega)$ (solid lines) and dynamic spin structure factor $\bar{S}_{\mathrm{S}}(k,\omega)$ (dotted lines) for a two-component Fermi gas with attractive interactions in a $I = 10$ lattice. The plots in the left hand column show the half-filling case $N_\uparrow = N_\downarrow = 5$, the ones in the right hand column are for $N_\uparrow = N_\downarrow = 4$. The interaction parameters for the different rows are $V/J = 0, -3, -6$, and -9 (from top to bottom). The bars at the forward edge of each plot represent the excitation spectrum.

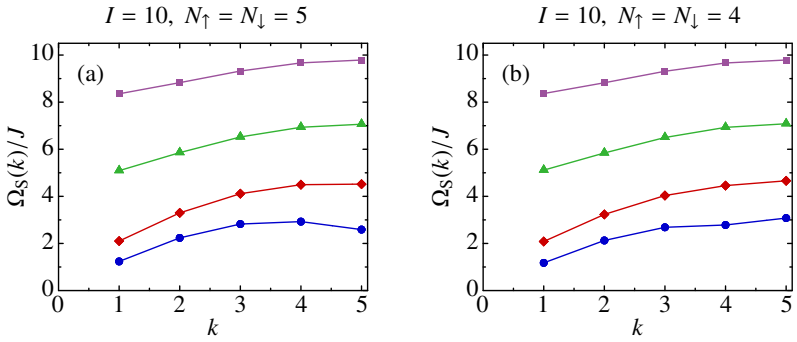

Figure 7. Centroid $\Omega_S(k)$ of the dynamic spin structure factor for a two-component Fermi gas with $N_\uparrow = N_\downarrow = 5$ (a) and $N_\uparrow = N_\downarrow = 4$ (b), resp., and attractive interactions $V/J = 0$ (●), -3 (♦), -6 (▲), and -9 (■).

$|V|$. The dynamic structure factor is also governed by this symmetry: The dynamic *density* structure factor $S_D(k,\omega)$ of a system with attractive interaction is identical to the dynamic *spin* structure factor $S_S(k,\omega)$ for a gas with a repulsive interaction of same magnitude.

The numerical results for the normalised dynamic density structure factor $\bar{S}_D(k,\omega)$ of the two-component fermionic system with attractive interactions are displayed in figure 6 (solid lines). The behaviour of the excitation strength is in stark contrast to the case of repulsive interactions. With growing attraction the strength is increasingly concentrated in one or two peaks at very low excitation energies. This effect does not depend on the filling as the comparison of the half-filling case (left hand column of figure 6) with a system away from half filling (right hand column) illustrates. The energy spectra are also largely independent of filling, for both fillings an energy gap appears for sufficiently strong attractive interactions. Remember, away from half-filling no mapping between density and spin sector exists anymore. The spectrum exhibits a gap for strong attractive interactions but no gap for repulsive interactions (cf. lower right hand panels in figures 4 and 6).

The appearance and the physical interpretation of the energy gap is related to pairing of the fermionic atoms due to the attractive interaction. This relation is revealed by the dynamic spin structure factor $S_S(k,\omega)$. As discussed in Ref. [11] for a homogeneous two-component Fermi gas, contributions to the spin structure factor arise from processes which break the pairs. Hence, the spin structure factor provides direct information on the pairing gap in the superconducting state. The dotted lines in figure 6 depict the spin structure factor. It is clearly seen that with increasing attraction the contributions to $S_S(k,\omega)$ are shifted towards larger energy transfers and that no low-lying strength remains. Eventually, as a gap in the energy spectrum appears, only those states above the gap contribute to the spin structure factor. As for the fermionic Mott-insulator the absence of low-lying strength implies the vanishing of the transition matrix elements $\langle \Psi_\nu^{\mathrm{FF}} | \hat{\rho}_{\mathrm{S}k}^\dagger | \Psi_0^{\mathrm{FF}} \rangle$ for all states below the gap. Notice, the spin-excitation gap is significantly larger than gap in the energy spectrum and it already appears for interaction strengths where the spectrum does not yet exhibit a gap.

We can use the centroid $\Omega_S(k)$ of the dynamic spin structure factor to characterise the gross features of spin excitations on the basis of sum rules. As for the Mott-insulator phase we can assess the existence and size of a spin-excitation gap already from the k-dependence of $\Omega_S(k)$ without ever calculating excited states. Figure 7 depicts the k-dependence of $\Omega_S(k)$ for the two fillings considered previously. Independent of the filling the centroid of the spin structure factor clearly shows the appearance of the spin-excitation gap already for weakly attractive interactions. As for the Mott-insulator we can use its behaviour for $k \to 0$ to

estimate the size of the excitation gap.

At half-filling the centroid of the spin structure factor depicted in panel (a) is identical to the centroid of the density structure factor for repulsive interactions of same magnitude (cf. figure 5) by virtue of the spin-density mapping. Away from half-filling this mapping does not apply and the behaviour of the centroids is completely different.

5. Summary

We have used the dynamic structure factor, a direct experimental observables, to pin-down signatures of the different zero-temperature quantum phases of single-component Bose and two-component Fermi gases in optical lattices. The systems are described within the single-band (Bose-) Hubbard model and we perform an exact diagonalisation of the Hamiltonian using Lanczos methods. Since we are interested mainly in generic signatures the computational restriction of this approach to moderate lattice sizes is of minor relevance. The important benefit of this exact approach is that all regions of the phase diagram can be addressed on the same footing.

The comparison of the full dynamic structure factor $S(k,\omega)$ for different interaction strengths and fillings exhibits clear signatures of the different quantum phases. The Mott-insulator phases in the bosonic and fermionic systems are associated with a finite excitation gap which grows linearly with V/J. That is, excitations in form of density fluctuations are possible only for energies ω larger than the excitation gap. Whereas the excitation gap in the bosonic system is directly determined by the gap between ground state and first excited state of the Hamiltonian, its origin in the two-component Fermi system is more involved. Many eigenstates of the Hamiltonian are available in the low-ω regime, however, they do not contribute to the excitation strength since their transition matrix elements for the fluctuation operator vanish. Hence, a clear distinction between excitation gap (for a particular type of excitation) and the gap in the eigenspectrum of the Hamiltonian is indispensable.

For the two-component Fermi gas with attractive interactions the dynamic spin structure factor indicates the onset of pairing between atoms of the different components. Similar to the density structure factor for the Mott-insulator phase, the spin structure factor exhibits an excitation gap. No spin fluctuations, which would require the breaking of a pair, are possible below an energy ω corresponding to the spin excitation gap. This phenomenon is independent of the total filling — unlike the Mott insulator — but requires equal population of the two components. The detailed nature of the pairing in the presence of attractive interactions will be discussed elsewhere.

Most of the physics revealed by the dynamic structure factors is already contained in integral quantities like the centroid of the strength distribution, which can be evaluated using sum rules. The knowledge of the ground state alone is sufficient to assess the appearance and size of excitation gaps. The explicit calculation of the excitation spectrum is required only if details of the dynamic structure factors are of interest. This paves the way towards predictions for larger system, e.g., within a Monte Carlo or Density Matrix Renormalisation Group approach, where the computation of the full excitation spectrum is not feasible.

Acknowledgements

This work was supported by the DFG, the UK EPSRC, and the EU via the “Cold Quantum Gases” network. K.B. thanks the Royal Society and Wolfson Foundation for support. R.R.

acknowledges fruitful discussions with Karen Braun-Munzinger, Jacob Dunningham, Markus Hild, and Felix Schmitt.

References

[1] M. Greiner, O. Mandel, T. Esslinger, *et al.*; Nature **415** (2002) 39.
[2] T. Stöferle, H. Moritz, C. Schori, *et al.*; Phys. Rev. Lett. **92** (2004) 130403.
[3] M. Greiner, O. Mandel, T. W. Hänsch, I. Bloch; Nature **419** (2002) 51.
[4] J. Stenger, S. Inouye, A. P. Chikkatur, *et al.*; Phys. Rev. Lett. **82** (1999) 4569.
[5] D. M. Stamper-Kurn, A. P. Chikkatur, A. Görlitz, *et al.*; Phys. Rev. Lett. **83** (1999) 2876.
[6] D. Jaksch, C. Bruder, J. I. Cirac, *et al.*; Phys. Rev. Lett. **81** (1998) 3108.
[7] A. Albus, F. Illuminati, J. Eisert; Phys. Rev. A **68** (2003) 023606.
[8] H. P. Büchler, G. Blatter; Phys. Rev. Lett. **91** (2003) 130404.
[9] M. Lewenstein, L. Santos, M. A. Baranov, H. Fehrmann; Phys. Rev. Lett. **92** (2004) 050401.
[10] R. Roth, K. Burnett; Phys. Rev. A **69** (2004) 021601.
[11] H.P. Büchler, P. Zoller, W. Zwerger; *Spectroscopy of Superfluid Pairing in Atomic Fermi Gases* (2004); e-Print: **cond-mat/0404116**.
[12] L. P. Pitaevskii, S. Stringari; *Bose-Einstein Condensation*; Oxford University Press, Oxford (2003).
[13] C. Menotti, M. Krämer, L. Pitaevskii, S. Stringari; Phys. Rev. A **67** (2003) 053609.
[14] A.-M. Rey, K. Burnett, R. Roth, *et al.*; J. Phys. B **36** (2003) 825.
[15] R. Roth, K. Burnett; Phys. Rev. A **67** (2003) 031602(R).
[16] R. Roth, K. Burnett; Phys. Rev. A **68** (2003) 023604.
[17] D. Pines, P. Nozieres; *The Theory of Quantum Liquids, Vol. I*; W. A. Benjamin, Inc., New York, Amsterdam (1966).
[18] G. G. Batrouni, R. T. Scalettar; Phys. Rev. B **46** (1992) 9051.
[19] J. K. Freericks, H. Monien; Phys. Rev. B **53** (1996) 2691.
[20] A. M. Rey, P. B. Blakie, G. Pupillo, *et al.*; *Bragg spectroscopy of ultracold atoms loaded in an optical lattice* (2004); e-Print: **cond-mat/0406552**.
[21] T. Giamarchi; *Quantum Physics in One Dimension*; Oxford University Press, Oxford (2004).